Subfemtosecond control of molecular fragmentation by hard X-ray photons.

O. Travnikova,[1,2,*] N. Sisourat,[1] T. Marchenko,[1,2] G. Goldsztejn,[1,†] R. Guillemin,[1,2] L. Journel,[1,2] D. Céolin,[2] I. Ismail,[1] A. F. Lago,[3] R. Püttner,[4] M. N. Piancastelli,[1,5] and M. Simon[1,2]

[1]*Sorbonne Universités, UPMC Univ Paris 06, CNRS, UMR 7614, Laboratoire de Chimie Physique-Matière et Rayonnement, F-75005 Paris, France*
[2]*Synchrotron SOLEIL, L'Orme des Merisiers, Saint-Aubin, BP 48, F-91192 Gif-sur-Yvette Cedex, France**
[3]*Centro de Ciências Naturais e Humanas, Universidade Federal do ABC (UFABC), 09210-170, Santo André, SP, Brazil*
[4]*Fachbereich Physik, Freie Universität Berlin, D-14195 Berlin, Germany*
[5]*Department of Physics and Astronomy, Uppsala University, SE-75120 Uppsala, Sweden*

(Dated: April 19, 2017)

Tuning hard X-ray excitation energy along Cl $1s \rightarrow \sigma^*$ resonance in gaseous HCl allows manipulating molecular fragmentation in the course of the induced multistep ultrafast dissociation. The observations are supported by theoretical modelling, which shows a strong interplay between the topology of the potential energy curves, involved in the Auger-cascades, and the so-called *core-hole-clock*, which determines the time, spent by the system in the very first step. Asymmetric profile of the fragmentation ratios reflects different dynamics of nuclear wave packets dependent on the photon energy.

PACS numbers: 33.80.Eh, 82.80.Pv, 31.50.Df, 82.53.-k

Creation of deep electron vacancies initiates a cascade of relaxation events that occurs on a timescale of few femtoseconds. In the case of molecules, ultrafast dissociation may take place in the course of such cascades. In a recent letter [1], we have described the mechanism of multi-step ultrafast dissociation (MUST UFD), induced by promotion of a deep inner-shell electron to an antibonding molecular orbital. Following the excitation, the system relaxes via a series of subsequent radiative or non-radiative (*i.e. Auger*) decay steps and passes through several repulsive intermediate states with one or more holes in the shallower core electron shells, which have longer lifetimes (typically 3–8 fs) compared to that of deep-core-hole states ($\leq$1 fs). MUST UFD process was demonstrated with the example of HCl following Cl $1s \rightarrow \sigma^*$ excitation. The intermediate Cl $2p^{-2}\sigma^*$ double-core-hole states with the lifetime of $\tau \leq 3$ fs are efficiently produced by the dominant *KLL* Auger decay channel and can dissociate by emitting a neutral hydrogen atom before the *LMM*1 Auger decay occurs. The H–Cl bond continues to elongate in the following doubly charged Cl $2p^{-1}(V\sigma^*)^{-2}$ core-hole states leading to more abundant fragmentation before the system relaxes by emitting another Auger electron in the last *LMM*2 decay step of the *KLL*-decay path:

$$\begin{aligned} h\nu + \mathrm{HCl} &\longrightarrow \mathrm{HCl}^*{}_{(1s^{-1}\sigma^*)} \xrightarrow{KLL} \\ &\xrightarrow{KLL\ (\tau_{eff} \lesssim 1\mathrm{fs})} \mathrm{HCl}^+{}_{(2p^{-2}\sigma^*)} + e^-_{Auger} \xrightarrow{LMM1} \\ &\xrightarrow{LMM1\ (\tau_1 \sim 3\mathrm{fs})} \mathrm{HCl}^{2+}{}_{(2p^{-1}(V\sigma^*)^{-2})} + e^-_{Auger} \xrightarrow{LMM2} \\ &\xrightarrow{LMM2\ (\tau_2 \sim 8\mathrm{fs})} \mathrm{HCl}^{3+}{}_{((V\sigma^*)^{-4})} + e^-_{Auger} \end{aligned}$$

In the present letter, we demonstrate that MUST UFD can be controlled by tuning the photon energy. Remarkably, this leads to drastic changes in nuclear dynamics, which are observed on the hundreds of attoseconds timescale.

The decay time of a core-excited state can be used as a reference clock (*'internal timer'*) for other processes occurring in the system. This is the heart of the well-known *core-hole clock method*, which has been successfully applied in soft-x-ray energy regime to the studies of ultrafast dissociation in isolated species taking place during the core-hole lifetime [2–19]. This method is the main tool in the the studies of charge transfer dynamics between adsorbates and surfaces [20–22], across adsorbate films between polymer chains [23], along single DNA chains [24]. Recently, it was used in the tender x-ray regime (2–10 keV) to observe subfemtosecond nuclear [25] and electron [26] dynamics in isolated molecules. It was also demonstrated that the core-hole clock method allows additionally to manipulate the time spent by the wave packet in the core-excited state through the *detuning* of the excitation energy from the maximum of the photoabsorption resonance – the so-called *'scattering time'*, or *'effective duration time'* [27]. The larger the mismatch (detuning, Ω) between the narrow-bandwidth photon energy and the vertical absorption energy, the shorter is the scattering duration time τ_{eff} due to the increased dephasing of the wave packet [28]. The mean scattering duration time can be approximated to:

$$\tau_{eff} \simeq 1/\sqrt{(\Omega^2 + \Gamma^2)}, \qquad (1)$$

where Γ is the lifetime broadening. The upper limit of the effective duration time is set by the lifetime of the core-hole state $\tau = \Gamma^{-1}$ when $\Omega = 0$. In the present case (a multi-step process), we control the dynamics of the overall Auger cascade by *manipulating* the effective scattering time of the very first step corresponding in our

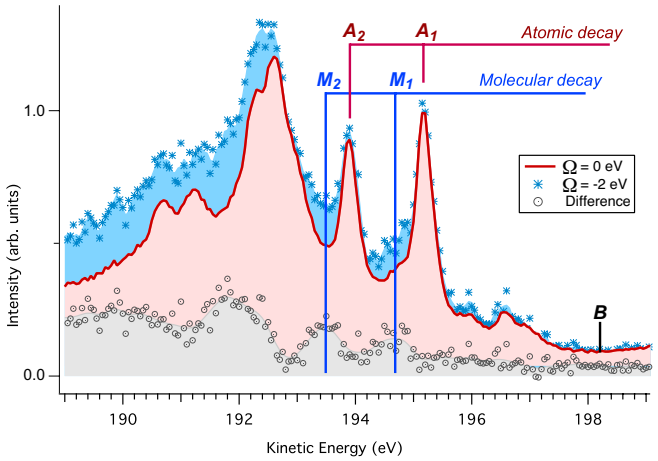

FIG. 1: Effect of photon energy detuning on $LMM1$ Auger decay spectra recorded for gaseous HCl on top of the Cl $1s \rightarrow \sigma^*$ resonance (red) and with detuning $\Omega = -2$ eV (blue). The sharp lines correspond to the atomic contributions after MUST UFD in the Cl $2p^{-2}\sigma^*$ double-core-hole states of HCl. The difference spectrum (grey) shows molecular contributions to the $LMM1$ Auger decay and is obtained by subtraction of the $\Omega = 0$ eV spectrum from the $\Omega = -2$ eV one in a way that atomic A_1 and A_2 lines disappear.

study to the decay of the Cl $1s^{-1}\sigma^*$ core-excited state, which is the shortest part ($\sim$1 fs) of the overall MUST UFD process (6–20 fs). Our observable is the amount of dissociation in the $LMM1$ step ($\tau_1 \sim$3 fs), which is monitored by the intensity of the atomic lines with respect to molecular background originating from the same electronic transition. Thus the *controlled* time (τ_{eff}) runs only up to about 25% of the scattering time for the second $LMM1$ step ($\tau_{eff} + \tau_1$) and less than 10% for the total scattering process ($\tau_{eff} + \tau_1 + \tau_2$).

In brief, during core-excitation a coherent nuclear wave packet is created in the primary core-excited state. This wave packet is formed with different initial conditions according to detuning, which determine its group velocity and, therefore, its evolution in the following relaxation steps. Afterwards, this detuning-dependent wave packet is promoted very fast to the lower intermediate state, where it has enough time to propagate towards the region of the dissociation to create the atomic peak.

The measurements have been performed on the GALAXIES beamline [29] at the 2.75 GeV SOLEIL synchrotron in France using the hard x-ray photoelectron spectroscopy (HAXPES) end-station [30]. In brief, the beamline delivers linearly polarized light, which is monochromatized by a Si(111) double crystal and focused by a toroidal mirror. The photon bandwidth is $\sim$250 meV around 3 keV. The HCl sample was commercially obtained from Air Liquide with a purity of >99%.

Resonant Auger spectra were recorded with a high-resolution EW4000 Scienta spectrometer equipped with wide-angle lens. The spectrometer is installed parallel to the light polarization vector. The electron spectrometer resolution is estimated to be $\sim$150 meV at 100 eV pass energy. Auger decay spectra were recorded at several photon energies across the Cl $1s \rightarrow \sigma^*$ resonance ($2823.8 \pm 2.0\ eV$). The full LMM Auger decay spectrum was the subject of a previous publication [1]. Figure 1 shows $LMM1$ part of the spectrum used in the discussion below. The two spectra, recorded for Ω=0 and -2 eV, shown in Fig. 1, are normalised to the intensity of the atomic peak (A_1) at $\sim$195 eV.

For the analysis, we chose the most intense atomic lines with highest kinetic energies corresponding to the $LMM1$ Auger decay of the Cl $2p^{-2}\sigma^*$ core-hole states of HCl (marked as A_1 and A_2 in Fig. 1). They correspond to $2p^4 3s^2 3p^6(^1D_2) \rightarrow 2p^5 3s^2 3p^4$(J=7/2, 5/2) transitions [31]. Their high intensity and rather isolated character makes them the most suitable for the study of the detuning effects. The shoulders on the low kinetic energy side of the atomic peaks are due to the broader molecular background originating from the early Auger decays occurring at small internuclear distances when the molecule is not yet dissociated (marked as M_1 and M_2 in Fig. 1). From Fig. 1, one can notice that the intensity in the region M_2 and the shoulder M_1 are more pronounced in the detuned blue spectrum for $\Omega = -2$ eV. This visually demonstrates that detuning of the photon energy from the maximum of the Cl $1s^{-1}\sigma^*$ resonance affects the nuclear dynamics and partially quenches the fragmentation in the following MUST UFD steps.

Furthermore, we tracked as a function of excitation energy across the resonance the variations of the intensity ratios for lines A_1 and A_2 versus their molecular counterparts M_1 and M_2 with respect to the overall background (marked as B in a flat region at the high kinetic energy side in Fig. 1). Peaks A_1 and A_2 were fitted to extract the peak maxima and the intensities of M_1, M_2 and B were determined as the mean values in the corresponding energy regions. The errors were estimated by propagation of experimental uncertainties. The observed experimental ratios are displayed in the middle panel of Fig. 2 as a function of the detuning Ω together with theoretical predictions (the upper panel).

Nuclear dynamics during the cascade was modelled using a semiclassical approach [1, 32]: classical trajectories are started on the Cl $1s^{-1}\sigma^*$ core-excited potential energy curve (PEC). Each trajectory is allowed to hop to the PECs of the Cl $2p^{-2}\sigma^*$ double-core-hole states according to the effective decay rate. After the first decay, the trajectories are further propagated on the new PEC and are allowed to decay according to the $LMM1$ lifetime τ_1. For each calculation, 40 000 trajectories were propagated until they decayed through $LMM1$ Auger transition. The atomic and molecular contributions to the $LMM1$ Auger spectra are taken as the number of trajectories hopping at distances above and below $2R_e$, respectively, where R_e is the equilibrium bond distance in

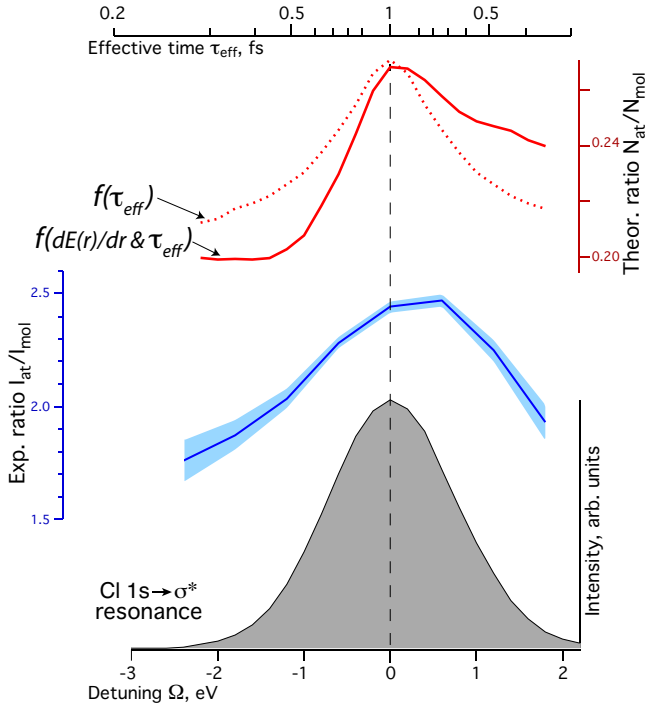

FIG. 2: Middle (in blue): experimental atomic-*versus*-molecular intensity ratio for MUST UFD in the Cl $2p^{-2}\sigma^*$ double-core-hole state of HCl following Cl $1s \rightarrow \sigma^*$ excitation using photon energies across the Cl $1s^{-1}\sigma^*$ resonance. Top (in red): theoretical atomic-*versus*-molecular ratio (including both τ_{eff} and $dE(r)/dr$ – full line; only τ_{eff} – dotted). Error bars are indicated by shaded areas. Bottom: Cl $1s \rightarrow \sigma^*$ partial electron yield spectrum (equivalent to X-ray absorption).

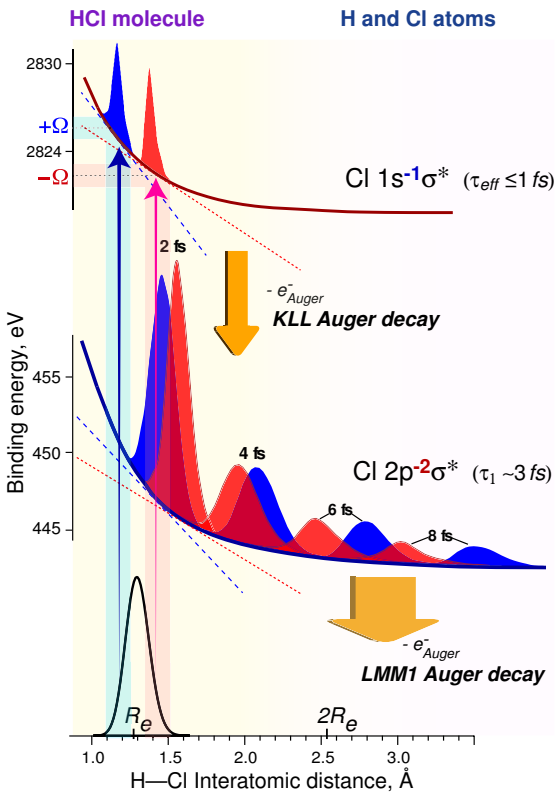

FIG. 3: Diagram describing the effect of the different energy gradients (dotted straight lines) on the wave-packet dynamics at the first two steps of the KLL Auger decay cascade path for positive (blue) and negative (red) detunings. The calculated initial (bottom), initially excited wave-packets (top) and their distributions in the Cl $2p^{-2}\sigma^*$ state after 2, 4, 6, 8 *fs* (middle).

the ground state HCl molecule. Same PECs and natural partial widths as in Ref. [1] were used.

For the relative atomic ratios, effective lifetimes for the Cl $1s^{-1}\sigma^*$ state were calculated using Eq. 1. In order to take the detuning effects into account, the initial conditions were chosen to reproduce the cross-section as

$$\sigma(\Omega) \propto \frac{|\chi_{\nu=0}(r)|^2}{(\Omega + E(R_e) - E(r))^2 + (\Gamma/2)^2} \qquad (2)$$

where $\chi_{\nu=0}(r)$ is the lowest vibrational wavefunction of the electronic ground state and $E(r)$ – the PEC of the core-excited state. Calculated relative atomic ratios were convoluted with Gaussian function of FWHM=250 meV, corresponding to the experimental photon bandwidth.

The observed atomic-*versus*-molecular ratio, i.e. the fraction of the photo-excited molecules undergoing dissociation, is asymmetric and with the centroid blue-shifted from the top of the Cl $1s \rightarrow \sigma^*$ resonance, where the effective duration scattering time is the longest (Eq. 1). To understand this apparent discrepancy, we looked in more details at the wave-packet dynamics at positive and negative detunings.

As depicted in Fig. 3, at positive detunings the part of the ground-state wave packet, residing at smaller internuclear distances, has higher probability to be promoted to the part of the Cl $1s \rightarrow \sigma^*$ state potential with larger gradients ($dE(r)/dr$), thus leading to large initial accelerations and fast velocity gains of the nuclei. Though τ_{eff} is the same for $\pm\Omega$, the accelerations of the nuclear wave packets are very different due to large variations of potential energy gradients at different internuclear distances. Previously, the effect of energy gradients upon detuning was discussed for single-step UFD induced by soft X-rays [5–8]. The relative atomic contributions were found to decrease approximately symmetrically upon detuning due to their predominant dependance on the effective duration of the resonant scattering [6, 8]. In a single-step UFD, the *total* duration is controlled by detuning (Eq. 1) and varies from Γ^{-1} to 0 ($\tau_{UFD} = \tau_{eff} \geq 0$). On the contrary, in MUST UFD only the very first step is detuning-dependent and the total duration never goes to zero, being always larger or equal to the sum of the lifetimes of all the following sequential steps. For example, for Cl $2p \rightarrow \sigma^*$ or Cl $1s \rightarrow \sigma^*$ resonances, when $\Omega = 2$ eV, the effective scattering time is ≈ 0.3 *fs* $\left(\text{both } \tau_{eff}(2p^{-1}) \text{ and } \tau_{eff}(1s^{-1})\right)$. The wave packet does not have time to spread in the Cl $1s^{-1}\sigma^*$

nor $2p^{-1}\sigma^*$ core-excited states. However, in the case of MUST UFD it decays to the Cl $2p^{-2}\sigma^*$ state of HCl, where the bond elongation continues during additional $\tau_1 = 3$ *fs*. Noteworthy, Cl $2p^{-2}\sigma^*$ states have even steeper potential energy curves than single core-hole states of HCl [1]. As a result, the bond dissociation occurs more efficiently for positive detunings due to higher $dE(r)/dr$ values of both Cl $1s^{-1}\sigma^*$ and Cl $2p^{-2}\sigma^*$ potential energy curves involved. At the moment of the $LMM1$ Auger decay, the estimated group velocity of the wave packet, corresponding to positive detuning of +2 eV, is almost 30% higher than that corresponding to the same negative detuning of –2 eV. It can be seen from Fig. 3 that in the Cl $2p^{-2}\sigma^*$ state the wave packet, corresponding to the positive detuning (marked as blue), takes over the wave-packet, corresponding to the negative detuning (marked as red), and reaches faster the bond distance of $2R_e$, where the molecule can be considered dissociated, despite the initial spatial distribution of the former at smaller H–Cl bond distances. As shown in Fig. 2 (upper panel), considering only the impact of the effective lifetime τ_{eff} leads to a symmetric atomic fragmentation ratio. Theory predicts strongly asymmetric dependence of atomic-*vs*-molecular ratios on detuning when including $dE(r)/dr$ dependence on the excitation energy in addition to the scattering time τ_{eff}.

The relative atomic ratios strongly depend on τ_{eff} of the Cl $1s^{-1}\sigma^*$ state only for moderate detunings $|\Omega| \lesssim 1$ eV (see dotted curve in Fig. 2). Variations in the ratios observed for $|\Omega| \gtrsim 1$ eV are mostly due to the topology of the potential energy curves and are dominated by the dynamics, occurring in the Cl $2p^{-2}\sigma^*$ state.

Notwithstanding negligible wave-packet movement during very short effective scattering times of the 1^{st} step of MUST UFD affected by detuning, the gained velocity is notable. For instance, while the relative displacement of the Cl $1s^{-1}\sigma^*$ core-excited wave packet is estimated to be less than 1% and almost 6% for $\Omega = -2/+2$ and 0 eV, respectively (τ_{eff} ∼300 *as* and 1 *fs*), the velocity, acquired on the Cl $1s^{-1}\sigma^*$ potential energy curve, amounts to 10%/12% and 36% of the corresponding final wave-packet velocities at the moment of the $LMM1$ Auger decay.

At large detunings (both positive and negative) the resonant photoabsorption cross section becomes small, thus the weight of direct contributions to molecular $LMM1$ Auger decays increases [27]. The direct terms are not included in our theoretical simulations of the wave-packet dynamics, which would partly explain the disagreement at large positive detunings, where experimental relative atomic ratios start to decrease rapidly, contrary to the simulations (Fig. 2).

In conclusion, the strongly dissociative character of the Cl $1s^{-1}\sigma^*$ state ($\tau \sim 1$ fs) leads to an important acceleration of the nuclei before the system decays into another dissociative and short-lived $2p^{-2}\sigma^*$ state of HCl ($\tau_1 \sim 3$ fs), where the H–Cl bond dissociation occurs. Detuning of the excitation photon energy from the maximum of the Cl $1s \rightarrow \sigma^*$ resonance results in the changes of dissociation rates. For example, detuning by -1 eV shortens the total scattering time by 400 attoseconds (10%), which is estimated to decrease by ∼20% the Auger decays occurring in already dissociated atomic fragments relative to molecular decays. On the other hand, positive detunings lead to a much lower decrease in the relative formation of atomic fragments. This is due to the interplay between potential energy gradients and the effective scattering time, which both depend on the excitation energy.

This interplay is very strong in the case of the Cl $1s \rightarrow \sigma^*$ excitation in HCl and must be a general phenomenon for the cascade relaxation processes. Detuning across dissociative resonances is predicted to allow manipulating the dynamics in the following multi-step decays by *"selecting"* different topologies of potential energy surfaces, especially when the core-hole clock is too fast to allow for displacements of the initially excited wave packet.

Experiments were performed on the GALAXIES beamline at SOLEIL Synchrotron, France (Proposals No. 20120122 and No. 99150133). We are grateful to SOLEIL staff for smoothly running the facility. A. F. L. thanks Coordenação de Aperfeiçoamento de Pessoal de Nível Superior-Brazil for the support. I.I. acknowledges financial support from Labex Plas@Par

* To whom correspondence should be addressed: oksana.travnikova@upmc.fr
† Present address: Max-Born-Institut, 12489 Berlin, Germany

[1] O. Travnikova, T. Marchenko, G. Goldsztejn, K. Jänkälä, N. Sisourat, S. Carniato, R. Guillemin, L. Journel, D. Céolin, R. Püttner, et al., Phys. Rev. Lett. **116**, 213001 (2016).
[2] P. Morin and I. Nenner, Phys. Rev. Lett. **56**, 1913 (1986).
[3] E. Kukk, H. Aksela, O.-P. Sairanen, S. Aksela, A. Kivimäki, E. Nõmmiste, A. Ausmees, A. Kikas, S. J. Osborne, and S. Svensson, J. Chem. Phys. **104**, 4475 (1996).
[4] F. Gel'mukhanov and H. Ågren, Phys. Rev. A **54**, 379 (1996).
[5] A. Menzel, B. Langer, J. Viefhaus, S. Whitfield, and U. Becker, Chem. Phys. Lett. **258**, 265 (1996).
[6] O. Björneholm, S. Sundin, S. Svensson, R. R. T. Marinho, A. Naves de Brito, F. Gel'mukhanov, and H. Ågren, Phys. Rev. Lett. **79**, 3150 (1997).
[7] E. Kukk, A. Wills, N. Berrah, B. Langer, J. D. Bozek, O. Nayadin, M. Alsherhi, A. Farhat, and D. Cubaynes, Phys. Rev. A **57**, R1485 (1998).
[8] A. Baev, P. Salek, F. Gel'mukhanov, H. Ågren, A. Naves de Brito, O. Björneholm, and S. Svensson, Chem. Phys. **289**, 51 (2003).

[9] F. K. Gel'mukhanov and H. Ågren, Appl. Phys. A **65**, 123 (1997).
[10] A. N. de Brito, A. N. de Brito, O. Björneholm, J. S. Neto, A. Machado, S. Svensson, A. Ausmees, S. J. Osborne, L. J. Sæthre, H. Aksela, et al., J. Mol. Struc.-THEOCHEM **394**, 135 (1997).
[11] E. Pahl, L. S. Cederbaum, H. D. Meyer, and F. Tarantelli, Phys. Rev. Lett. **80**, 1865 (1998).
[12] P. Sałek, F. Gel'mukhanov, and H. Ågren, Physical Review A **59**, 1147 (1999).
[13] O. Björneholm, M. Bässler, A. Ausmees, I. Hjelte, R. Feifel, H. Wang, C. Miron, M. N. Piancastelli, S. Svensson, S. L. Sorensen, et al., Phys. Rev. Lett. **84**, 2826 (2000).
[14] I. Hjelte, M. N. Piancastelli, R. F. Fink, O. Björneholm, M. Bässler, R. Feifel, A. Giertz, H. Wang, K. Wiesner, A. Ausmees, et al., Chem. Phys. Lett. **334**, 151 (2001).
[15] K. Wiesner, A. Naves de Brito, S. L. Sorensen, F. Burmeister, M. Gisselbrecht, S. Svensson, and O. Björneholm, Chem. Phys. Lett. **354**, 382 (2002).
[16] I. Hjelte, M. N. Piancastelli, C. M. Jansson, K. Wiesner, O. Björneholm, M. Bässler, S. L. Sorensen, and S. Svensson, Chem. Phys. Lett. **370**, 781 (2003).
[17] K. Le Guen, C. Miron, D. Céolin, R. Guillemin, N. Leclercq, M. Simon, P. Morin, A. Mocellin, O. Björneholm, A. Naves de Brito, et al., J. Chem. Phys. **127**, 114315 (2007).
[18] O. Travnikova, V. Kimberg, R. Flammini, X.-J. Liu, M. Patanen, C. Nicolas, S. Svensson, and C. Miron, J. Phys. Chem. Lett. **4**, 2361 (2013).
[19] H. Sann, T. Havermeier, C. Müller, H. K. Kim, F. Trinter, M. Waitz, J. Voigtsberger, F. Sturm, T. Bauer, R. Wallauer, et al., Phys. Rev. Lett. **117**, 243002 (2016).
[20] P. A. Brühwiler, O. Karis, and N. Mårtensson, Rev. Mod. Phys. **74**, 703 (2002).
[21] A. Fohlisch, P. Feulner, F. Hennies, A. Fink, D. Menzel, D. Sanchez-Portal, P. M. Echenique, and W. Wurth, Nature **436**, 373 (2005).
[22] D. Menzel, Chem. Soc. Rev. **37**, 2212 (2008).
[23] C. Arantes, B. G. A. L. Borges, B. Beck, G. Araújo, L. S. Roman, and M. L. M. Rocco, J. Phys. Chem. C **117**, 8208 (2013).
[24] H. Ikeura-Sekiguchi and T. Sekiguchi, Phys. Rev. Lett. **99**, 228102 (2007).
[25] M. N. Piancastelli, G. Goldsztejn, T. Marchenko, R. Guillemin, R. K. Kushawaha, L. Journel, S. Carniato, J.-P. Rueff, D. Céolin, and M. Simon, J. Phys. B **47**, 124031 (2014).
[26] T. Marchenko, S. Carniato, L. Journel, R. Guillemin, E. Kawerk, M. Žitnik, M. Kavčič, K. Bučar, R. Bohinc, M. Petric, et al., Phys. Rev. X **5**, 031021 (2015).
[27] F. Gel'mukhanov and H. Ågren, Phys. Rep. **312**, 87 (1999).
[28] F. Gel'mukhanov, P. Sałek, T. Privalov, and H. Ågren, Phys. Rev. A **59**, 380 (1999).
[29] J.-P. Rueff, J. M. Ablett, D. Céolin, D. Prieur, T. Moreno, V. Balédent, B. Lassalle-Kaiser, J. E. Rault, M. Simon, and A. Shukla, J. Synchrotron Radiat. **22**, 175 (2015).
[30] D. Céolin, J. M. Ablett, D. Prieur, T. Moreno, J. P. Rueff, T. Marchenko, L. Journel, R. Guillemin, B. Pilette, T. Marin, et al., J. Electron Spectrosc. Relat. Phenom. **190**, 188 (2013).
[31] F. von Busch, U. Kuetgens, J. Doppelfeld, and S. Fritzsche, Phys. Rev. A **59**, 2030 (1999).
[32] N. Sisourat, J. Chem. Phys. **139**, 074111 (2013).